

Dynamic Performance Prediction of Brushless Resolver

D. Arab-Khaburi*, F. Tootoonchian* and Z. Nasiri-Gheidari**

Abstract: A mathematical model based on d-q axis theory and dynamic performance characteristic of brushless resolvers is discussed in this paper. The impact of rotor eccentricity on the accuracy of position in precise applications is investigated. In particular, the model takes the stator currents of brushless resolver into account. The proposed model is used to compute the dynamic and steady state equivalent circuit of resolvers. Finally, simulation results are presented. The validity and usefulness of the proposed method are thoroughly verified with experiments.

Keywords: Brushless Resolver, Dynamic Performance, Simulation, Steady State Behavior.

1 Introduction

In advanced control methods such as vector control, rotor position and its speed must be known instantaneously. This can be achieved by using either an optical encoder or a resolver. In many applications, a resolver is the preferred choice because of its mechanical ruggedness, reliability and its ability to reject the common mode noise [1-4]. A resolver is an electromagnetic rotational transducer that detects angular displacements. It is easy to integrate with the motor system [5-6]. A typical brushless resolver is composed of two parts: Rotary Transformer and traditional resolver. There are two windings in the rotary transformer: primary (in stator) and secondary (in rotor) [7]. The rotary transformer transfers the exciting signal to rotating part and applies it to the primary winding of the resolver [8-9]. A traditional resolver has three windings, the first one is used as the excitation winding, and the other two, which are spaced 90° from each other, are the outputs. The induced voltages in the output windings contain rotor position information. Simplified dynamic equations of resolver were presented in [10], but the impact of eccentricity and stator currents were not considered, and sinusoidal steady state behavior was not studied. Another method in [11], based on magnetic field analysis, determines an optimal magnetic design, using 2-D FEM (two-dimensional finite element method) and includes eccentricity, but its computing process is time consuming.

The objective of this paper is to present a mathematical model based on d-q axis theory to predict the dynamic and static behavior of a brushless resolver, considering eccentricity effect. This model gives us the dynamic and static equivalent circuit for resolvers. The advantages of the proposed approach are simplicity, accuracy and less computation time.

The rest of this paper is organized as following: We present the resolver model in Section 2. The simulation model is explained in Section 3. Results of our experiments are discussed in Section 4, and conclusions are presented in Section 5.

2 Resolver Model

The resolver model proposed in this paper is based on d-q axis theory. The following assumptions are considered in the analysis:

- Stator is assumed to have sinusoidal distributed polyphase windings.
- Rotor has a winding with sinusoidal supply.
- the model of resolver is obtained by assuming different resolver permeances in d-q axis.

Fig. 1 shows the model of a resolver. Each stator winding flux consists of leakage flux and main flux, the latter flux links the rotor [12].

2.1 Dynamic Model

The voltage equations in machine variables may be expressed as following:

$$\begin{aligned} V_r = & r_r i_r + L_{rr} \frac{di_r}{dt} + \omega_r L_{sr} \cos \theta_r i_{as} + L_{sr} \sin \theta_r \frac{di_{as}}{dt} \\ & + \omega L_{sr} \sin \theta_r i_{bs} - L_{sr} \cos \theta_r \frac{di_{bs}}{dt} \end{aligned} \quad (1)$$

Iranian Journal of Electrical & Electronic Engineering, 2008.

Paper first received 13th June 2007 and in revised form 5th May 2008.

* Davood Arab-Kahburi and Farid Tootoonchian are with the Department of Electrical Engineering, Iran University of Science and Technology, Tehran, Iran.

E-mail: kaburi@iust.ac.ir, tootoonchian@iust.ac.ir.

** Zahra Nasiri-Gheidari is with the Department of Electrical Engineering, Sharif University of Technology, Tehran, Iran.

E-mail: z_nasiri@ee.sharif.edu.

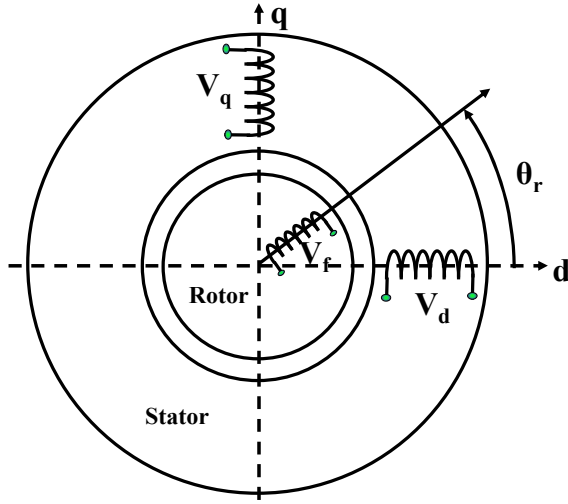


Fig. 1 Resolver model [12].

$$V_{as} = -r_s i_{as} + 2\omega_r L_{ms} \sin 2\theta_r i_{as} + L_{ms} \sin 2\theta_r \frac{di_{bs}}{dt} - 2\omega_r L_{ms} \cos 2\theta_r i_{bs} - L_{sr} \sin \theta_r \frac{di_r}{dt} \quad (2)$$

$$V_{bs} = -r_s i_{bs} - 2\omega_r L_{ms} \cos 2\theta_r i_{as} - L_{ms} \sin 2\theta_r \frac{di_{as}}{dt} - 2\omega_r L_{ms} \sin 2\theta_r i_{bs} + \omega_r L_{sr} \sin \theta_r i_r + (L_{\ell s} + L_0 + L_{ms} \cos 2\theta_r) \frac{di_{bs}}{dt} - L_{sr} \cos \theta_r \frac{di_r}{dt} \quad (3)$$

In the above equations the s subscript denotes variables and parameters associated with the stator circuits, and the r subscript denotes variables and parameters associated with the rotor circuit. V_{as} , V_{bs} are the stator voltages, V_r is the excitation signal of the resolver ($V_r = V'_r \cos(\omega_r t + \psi)$). i_{as} , i_{bs} are the stator currents, i_r is the rotor current r_s is the resistance of stator circuit; $L_{\ell s}$, L_{ms} are, respectively, the leakage and magnetizing inductances of the stator winding; r_r , L_{rr} are the resistance and inductance of rotor circuit, L_{sr} is the mutual inductance between the rotor and stator circuits, ω_r is the rotor angular frequency and θ_r is electrical angular displacement.

The stator variables are transferred to the rotor reference frame which eliminates the time-varying inductances in the voltage equations. Park's equations are obtained by setting the speed of the stator frame equal to the rotor speed.

The expressions for the flux linkages are:

$$\begin{aligned} \lambda_q &= (L_{\ell s} + L_0 - L_{ms}) i_q = (L_{\ell s} + L_{mq}) i_q \\ \lambda_d &= (L_{\ell s} + L_0 + L_{ms}) i_d + L_{md} i_r = (L_{\ell s} + L_{md}) i_d + L_{md} i_r \\ \lambda_r &= L_{md} i_d + (L_{\ell r} + L_{md}) i_r \end{aligned} \quad (4)$$

and

$$\begin{aligned} \psi &= \omega_b \lambda \\ x &= \omega_b L \end{aligned} \quad (5)$$

then

$$\begin{aligned} \psi_q &= (X_{\ell s} + X_{mq}) i_q = X_{\ell s} i_q + \psi_{mq} \\ \psi_d &= (X_{\ell s} + X_{md}) i_d + X_{md} i_r = X_{\ell s} i_d + \psi_{md} \\ \psi_r &= X_{md} i_d + (X_{\ell r} + X_{md}) i_r = X_{\ell r} i_r + \psi_{md} \end{aligned} \quad (6)$$

By referring rotor variables to the stator windings, voltage equations will be:

$$\begin{aligned} V_q &= -r'_s i_{qs} + \frac{1}{\omega_b} \frac{d\psi_q}{dt} + \frac{\omega_r}{\omega_b} \psi_d \\ V_d &= -r'_s i_{ds} + \frac{1}{\omega_b} \frac{d\psi_d}{dt} - \frac{\omega_r}{\omega_b} \psi_q \\ V'_r &= r'_r i'_r + \frac{1}{\omega_b} \frac{d\psi'_r}{dt} \end{aligned} \quad (7)$$

In order to obtain the equivalent circuits, the flux linkages per second in equation (7) should be replaced by currents. Thus, the voltage-current equations are as following:

$$\begin{bmatrix} V_q \\ V_d \\ V'_r \end{bmatrix} = \begin{bmatrix} -r'_s + \frac{p}{\omega_b} X_q & \frac{\omega_r}{\omega_b} X_d & \frac{\omega_r}{\omega_b} X_{md} \\ -\frac{\omega_r}{\omega_b} X_q & -r'_s + \frac{p}{\omega_b} X_d & \frac{p}{\omega_b} X_{md} \\ 0 & \frac{p}{\omega_b} X_{md} & r'_r + \frac{p}{\omega_b} X'_{rr} \end{bmatrix} \times \begin{bmatrix} i_q \\ i_d \\ i'_r \end{bmatrix} \quad (8)$$

where:

$$\begin{aligned} X_q &= X_{\ell s} + X_{mq}, X_{mq} = X_0 - X_{ms} \\ X_d &= X_{\ell s} + X_{md}, X_{md} = X_0 + X_{ms} \end{aligned} \quad (9)$$

and p is d/dt [12].

The electrical equivalent circuits of the resolver are presented in Fig. 2.

The electromagnetic torque developed in the resolver is given by:

$$T_{em} = \frac{P}{2\omega_b} (\psi_d i_q - \psi_q i_d) \quad (10)$$

and the mechanical equation of resolver in per unit can be written as:

$$T_{em}(\text{pu}) + T_{mech}(\text{pu}) - T_{damp}(\text{pu}) = 2H \frac{d(\frac{\omega_r}{\omega_b})}{dt} \quad (11)$$

where H is inertia constant expressed in second, T_{mech} is load torque and T_{damp} is fractional torque.

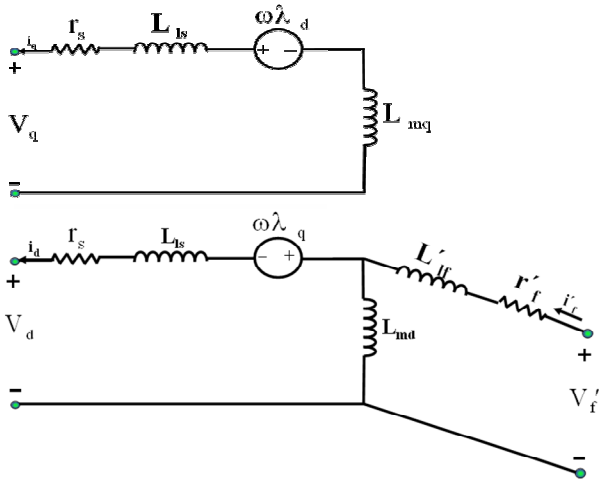


Fig. 2 Dynamic electrical equivalent circuits of the resolver.

2.2 Steady State Model

In steady state, the electrical angular velocity of the rotor is constant and equals to ω_e . In this mode of operation the rotor windings do not experience any change of flux linkages [14]. Thus, with ω_r set equal to ω_e and the time rate of change of all flux linkages neglected, the steady state versions of (7) and (8) become:

$$\begin{aligned} V_q^e &= V_q = -r_s I_q - \frac{\omega_e}{\omega_b} X_d I_d + \frac{\omega_e}{\omega_b} X_{md} I_r' \\ V_d^e &= V_d = -r_s I_d + \frac{\omega_e}{\omega_b} X_q I_q \\ V_r'^e &= V_r' = -r_r I_r' \end{aligned} \quad (12)$$

Here the ω_e to ω_b ratio is again included to accommodate analysis when the operation frequency is other than rated. In the synchronously rotating reference frame and using uppercase letters to denote the constant steady state variables [14]:

$$\sqrt{2}\tilde{F}_{as} = F_{qs}^e - jF_{ds}^e \quad (13)$$

where, F is each electrical variable (voltage, current, flux linkage), \tilde{F}_{as} is a phasor which represents a sinusoidal quantity; F_{qs}^e and F_{ds}^e are real quantities representing the constant steady state variables of the synchronously rotating reference frame. Hence

$$\sqrt{2}\tilde{V}_{as} = V_q^e - jV_d^e \quad (14)$$

Substituting (12) into (14) yields:

$$\begin{aligned} \sqrt{2}\tilde{V}_{as} &= -\left[r_s + \frac{\omega_e}{\omega_b} X_q \right] \tilde{I}_d \\ &+ \frac{1}{\sqrt{2}} \left[-\frac{\omega_e}{\omega_b} (X_d - X_q) I_d + \frac{\omega_e}{\omega_b} X_{md} I_r' \right] \end{aligned} \quad (15)$$

For symmetrical resolver, $X_d = X_q$ and $\omega_e = \omega_b$. So (15) can be write as:

$$\begin{aligned} \tilde{V}_{as} &= -(r_s + jX_s) \tilde{I}_{as} + \tilde{E}_a \\ \tilde{E}_a &= \frac{1}{\sqrt{2}} X_m I_r' \end{aligned} \quad (16)$$

where

$$X_s = X_{ls} + X_m \quad (17)$$

Considering above equations, the steady state equivalent circuit of resolver is shown in Fig. 3.

3 Simulation

The state equations on the rotating d-q reference frame are introduced. MATLAB/Simulink software is used for simulation.

Input, output and state variables are:

$$\begin{aligned} \text{StateVariables} &= [\psi_{qs}, \psi_{ds}, \psi_r'] \\ \text{InputVector} &= [V_r', \Delta T_{mech}] \\ \text{OutputVector} &= [\Delta \theta_r] \end{aligned}$$

In generalized theory of electrical machinery, it is more convenient to use flux linkages as the state variables [14-15]. By this way, the differential operators change to integral operators. Using Equation (6) and (8), the flux-linkages equations could be obtained as follow:

$$\psi_q = \omega_b \int \left(V_q + \frac{r_s}{X_{ls}} (-\psi_{mq} + \psi_q) - \frac{\omega_r}{\omega_b} \psi_d \right) dt \quad (18)$$

$$\psi_d = \omega_b \int \left(V_d + \frac{r_s}{X_{ls}} (-\psi_{md} + \psi_d) + \frac{\omega_r}{\omega_b} \psi_q \right) dt \quad (19)$$

$$\psi_r' = \omega_b \int \left(V_r' + \frac{r_r'}{X_{lr}} (\psi_{md} - \psi_r') \right) dt \quad (20)$$

where

$$\psi_{md} = \left(\frac{1}{X_{md}} + \frac{1}{X_{lr}} + \frac{1}{X_{ls}} \right)^{-1} \left(\frac{\psi_d}{X_{ls}} + \frac{\psi_r'}{X_{lr}} \right) \quad (21)$$

$$\psi_{mq} = \left(\frac{1}{X_{mq}} + \frac{1}{X_{ls}} \right)^{-1} \frac{\psi_q}{X_{ls}} \quad (22)$$

And angular position, stator and rotor current can be calculated as:

$$\theta(t) = \delta(t) = \theta_r(t) - \theta_e(t) = \int_0^t (\omega_r - \omega_e) dt + \theta_r(0) - \theta_e(0) \quad (23)$$

$$i_q = \frac{\Psi_q - \Psi_{mq}}{X_{\ell s}} \quad (24)$$

$$i_d = \frac{\Psi_d - \Psi_{md}}{X_{\ell s}} \quad (25)$$

$$i'_r = \frac{\Psi'_r - \Psi_{rd}}{X'_{\ell r}} \quad (26)$$

It must be mentioned that the proposed model can consider the eccentricity in a resolver, by taking into account a difference between L_d and L_q [11,13]. Fig. 4 shows a block diagram which simulates the resolvers.

4 Results and Discussions

Fig. 5 shows the resolver and its experimental setup. This resolver is a pancake type, and its specifications are presented in Table 1. Parameters of resolver's equivalent circuit, are given in Appendix I. This resolver was tested using a 100 watt, 12000 r.p.m. DC motor.

The input resistance of R/D converter is very high and the current in the resolver's stator coils, which apply to the R/D converter, is about micro ampere [16].

Fig. 6 shows resolver's test conditions, nominal frequency (4 KHz) and 60 μ A ($5 \times$ conventional R/D Nominal Current) stator output currents.

Table 2 shows the comparison of simulated and experimental output voltages. Results show good agreement between test and simulation voltages (about 1.19% error).

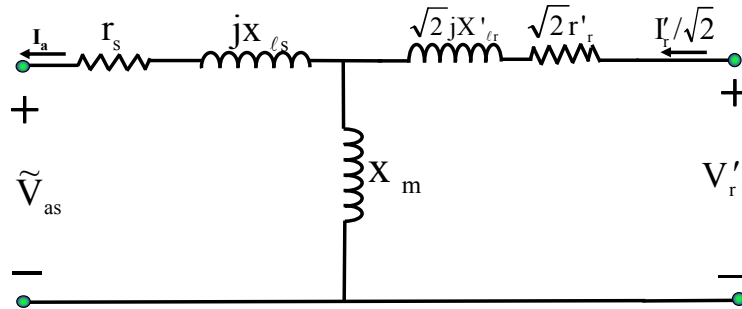


Fig. 3 Steady state equivalent circuits of the resolver.

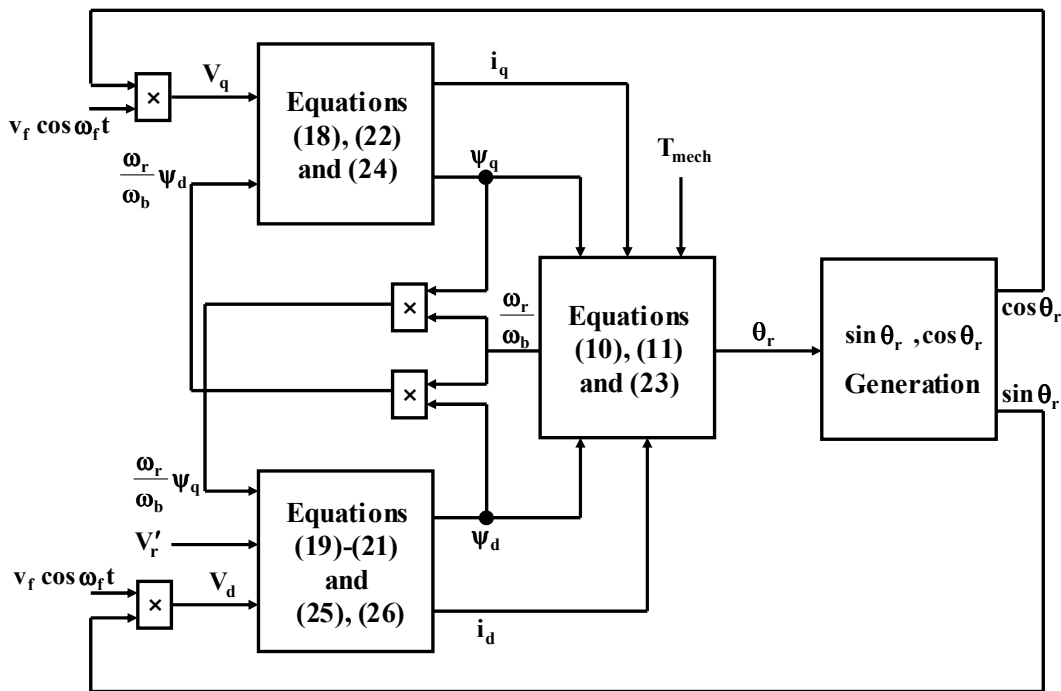
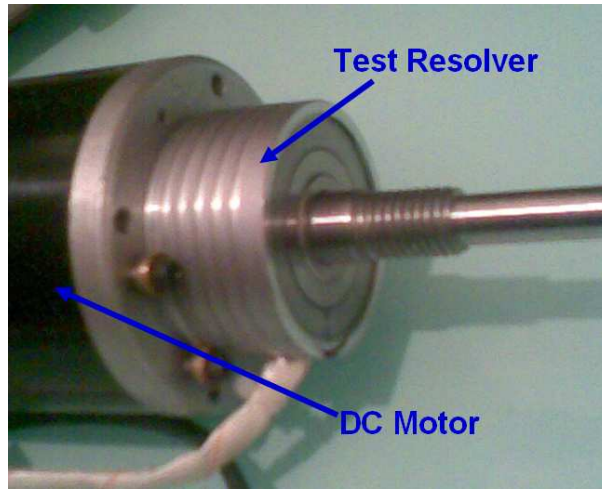


Fig. 4 Block diagram of resolver simulation.



(a)



(b)

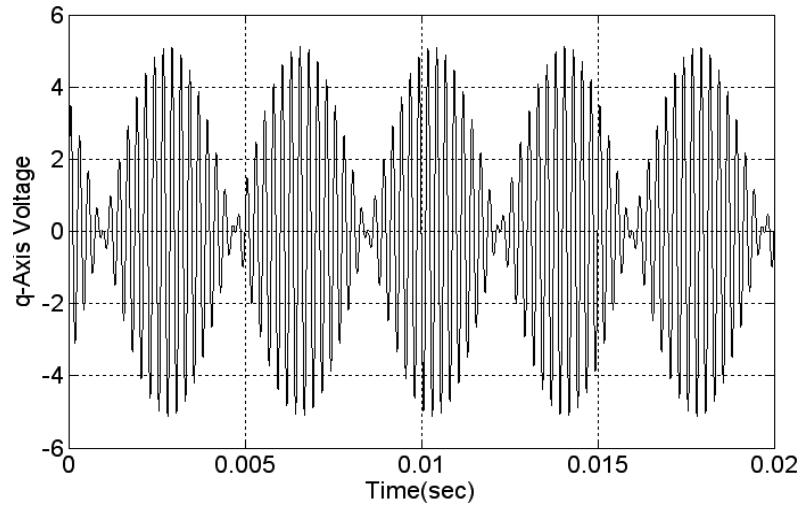
Fig. 5 (a) Manufactured resolver, (b) Experimental setups of the test resolver.

Table 1 Specifications of tested resolver.

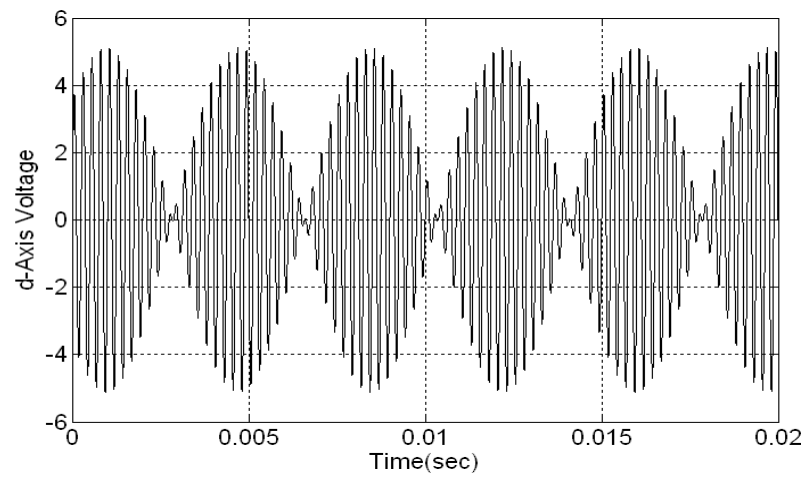
| | |
|------------------------------|----------------|
| Input voltage (rms) | 7.07 V |
| Output voltage (rms) | 3.53 V |
| Maximum position error (min) | 10 min |
| Maximum angular speed (rpm) | 8000-12000 rpm |
| Duty Cycle | S1 |
| Pole number | 2 |

For practical test a rotary tycope that connected to VF5-HP20 CNC Machine (Computer Numeric Control) is used. Different rotary positions are produced by this tycope in $[0, 2\pi]^{\text{rad}}$. Resolver output and simulation

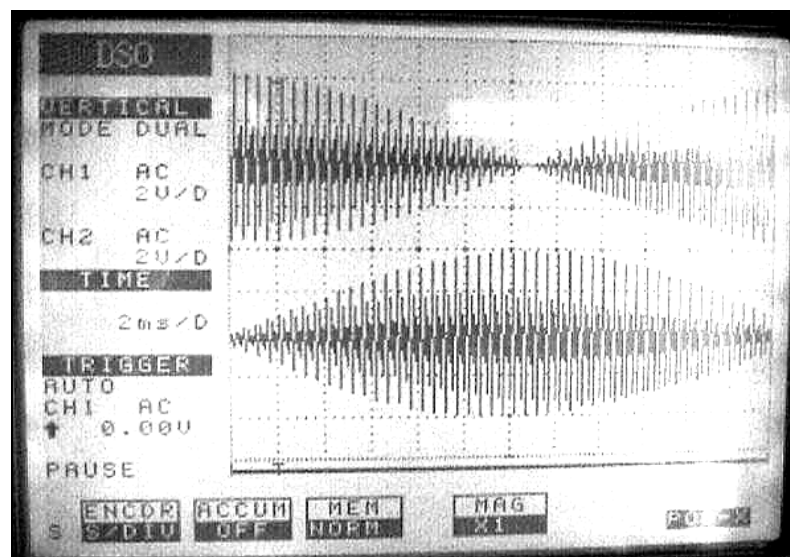
result are compared in each of these positions (The resolver output is obtained from arctangent of output voltages ratio).



(a)



(b)



(c)

Fig. 6 Output voltage of resolver versus time with 4 kHz excitation and 60 μ A output currents, (a) simulated q-axis voltage, (b) simulated d-axis voltage, and (c) measured q-d axis voltages.

Table 2 Comparisons of calculated and measured results.

| Output current (mA) | Frequency (Hz) | Output voltage (simulated) | Output voltage (measured) | Error (%) |
|---------------------|----------------|----------------------------|---------------------------|-----------|
| 0.060 | 4000 | 5 | 5.06 | 1.19 |

Fig. 7 shows the comparisons of simulation results with resolver output position. This figure shows the maximum position error is ± 3 Arcmin.

In proposed model d-q axis inductances are different parametric variables. By using unequal values for L_d , L_q eccentricity of resolver will be modeled.

Fig. 8 shows the eccentric resolver output voltages and angular position. Considering equations (2), (3); the resolver's peak induced voltages aren't influenced from eccentricity. Comparison of figures 6(a),(b) and 8(a),(b) confirms this effect. But the voltage phases are shifted. This phase shifting affects the detected angular position accuracy. Symmetric and eccentric resolver outputs are shown in Fig. 9.

This figure shows rotor eccentricity about 0.175 mm (50% gap eccentricity) causes 18.1 Arcdeg. error in detected angular position.

There are different methods for this error elimination that may be introduced in other papers. We have studied a new method based on resolver eigenvalues that will be published soon.

5 Conclusions

In this paper, a brushless resolver was analyzed. Its dynamic and steady state equivalent circuits were presented for the first time. Proposed model is taking the eccentricity effect (By using different parametric inductance on q-d axis) and stator currents into account. Comparison between experimental and simulation results shows 1.19% error in output voltages, and ± 3 Arcmin error in detected angular position. These results demonstrated the accuracy of the proposed model for resolvers. Because of model's ability in predicting eccentricity, the effect of 50% gap eccentricity was studied in stator voltages and detected angular position.

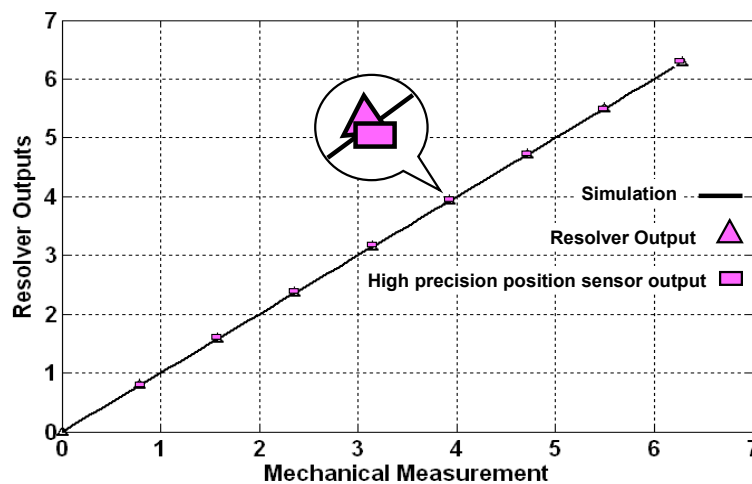
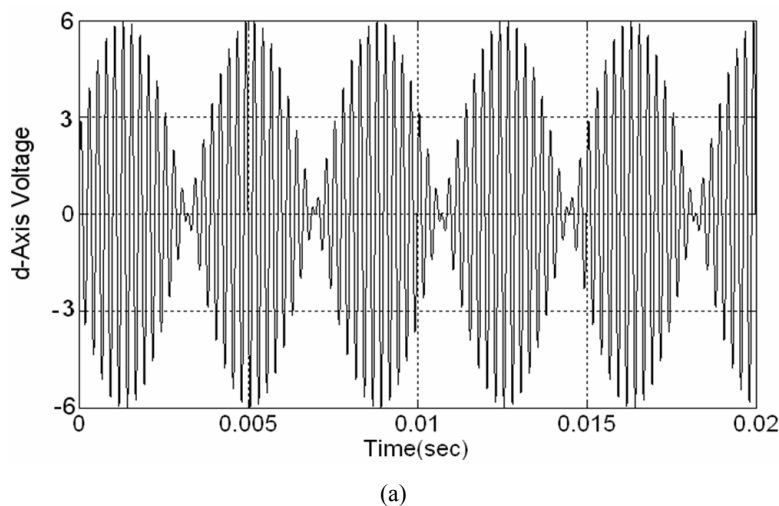
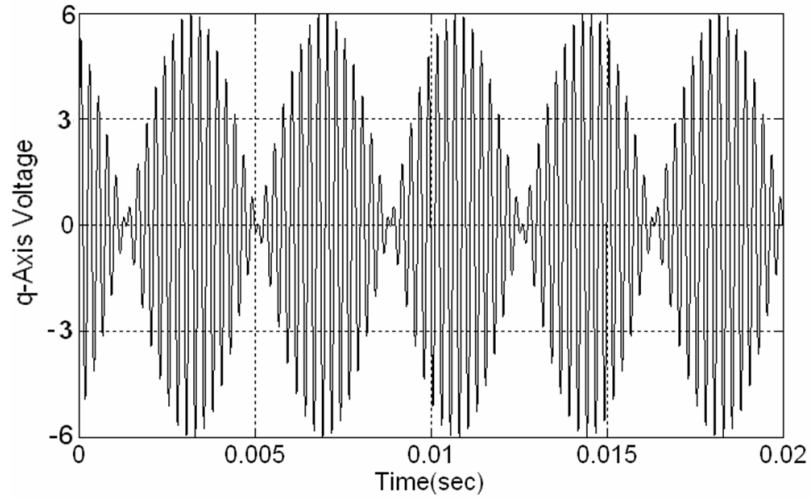
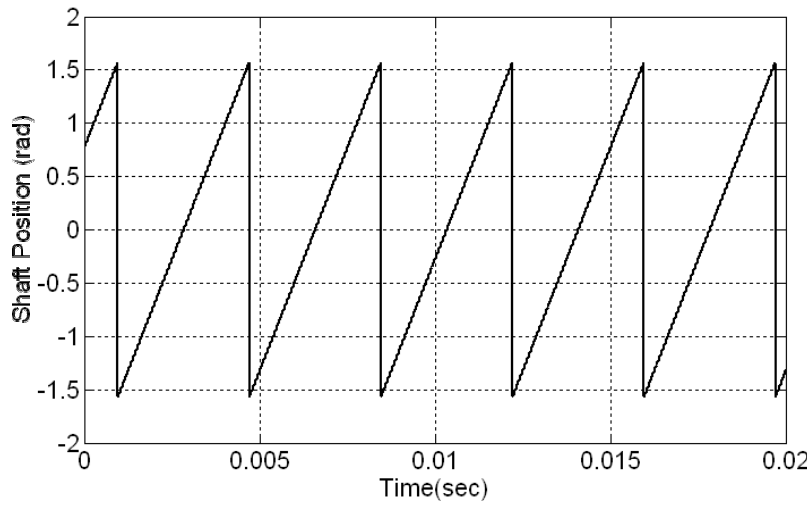


Fig. 7 Comparison of calculated angular position with resolver output and tycope output.





(b)



(c)

Fig. 8 Output voltage of eccentric resolver versus time with 4 KHz excitation, (a) d-axis voltage, (b) q-axis voltage, and (c) angular position.

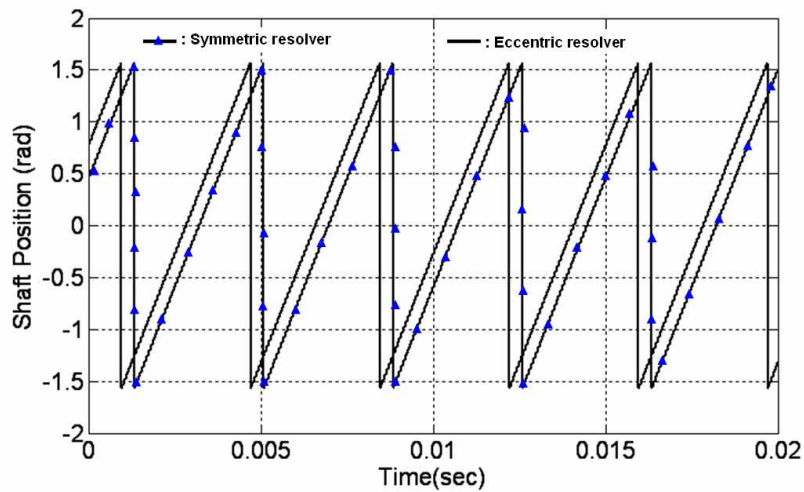


Fig. 9 Comparison of angular position in eccentric and symmetric resolver.

Appendix

The test resolver equivalent circuit parameters are presented at Table I.

Table I Equivalent circuit parameter of tested resolver.

| | |
|-------------------------|------------------------|
| r_s [Ω] | 40 |
| L_{ls} [H] | 0.2×10^{-3} |
| L_m [H] | 2.089×10^{-3} |
| r'_r [Ω] | 19 |
| L'_{lr} [H] | 0.2×10^{-3} |
| J [Kg.m^2] | 1.24×10^{-4} |

References

- [1] Choong-Hyuk Y., Ha I. and Ko M., "A Resolver-to-Digital Conversion Method for Fast Tracking," *IEEE Trans. On Industrial Electronics*, Vol. 39, pp. 369-378, Oct. 1992.
- [2] Munay B. A., Li. W. D., "A Digial Tracking R/D Converter with Hardware Error Calculation Using a TMS320C14," *Fifth European Conference on Power Electronics and Applications*, pp. 472-477, 13-16 Sept. 1993.
- [3] Hanselman D. C., "Techniques for Improving Resolver-to-Digital Conversion Accuracy," *IEEE Trans. on Industrial Electronics*, Vol. 38, No. 6, pp. 501-504, Dec. 1991.
- [4] Axsys Company R&D Group, *Pancake Resolvers Handbook*, <http://www.Axsys.com>, received at 15 December 2006.
- [5] Hanselman D. C., Thibodeau R. E. and Smith D. J., "Variable-reluctance Resolver Design Guidelines," *IEEE IECON*, New York, pp. 203-208, 1989.
- [6] Sun L. Z., Zou J. B. and Lu Y. P., "New Variable-reluctance resolver for Rotor-position sensing," *IEEE conference*, pp. 5-8, 2004.
- [7] Bünt A., Beinek S., "High-Performance Speed Measurement by Suppression of Systematic Resolver and Encoder Errors," *IEEE Trans. on Industrial Electronics*, Vol. 51, No. 1, pp. 49-53, Feb. 2004.
- [8] Huang Y., Chen Ch. and Shu W., "Finite Element Analysis on Characteristics of Rotary Transformers," *IEEE Trans. on Magnetics*, Vol. 30, No. 6, pp. 4866-4868, Nov. 1994.
- [9] Inoue H., Fusayasu H. and Takahari N., "Investigation of Factors Affecting Crosstalk in a Rolary Transformer," *IEEE Trans. on Magnetics*, Vol. 33, No 2, pp. 2215-2218, March 1997.
- [10] Jiuqing W., Xingshan L. and Hong G., "The Analysis and Design of High-speed Brushless Resolver plus R/D Converter Shaft-angle Measurement system," *IEEE conference*, pp. 289-292, 2000.
- [11] Masaki K., Kitazawa K., Mimura H., Nirei M., Tsuchimichi K., Wakiwaka H. and Yamada H., "Magnetic field analysis of a resolver with a skewed and eccentric rotor," *Elsevier trans. on Sensors and Actuators*, Vol. 81, pp. 297-300, 2000.
- [12] Arab-Khaburi D., Tootoonchian F., Nasiri-Gheidari Z., "Parameter identification of a brushless resolver using charge response of stator current," *Iranian Journal of Electrical & Electronic Engineering*, Vol. 3, Nos. 1&2, pp. 42-52, Jan. 2007.
- [13] Masaki K., Kitazawa K., Mimura H., Tsuchimichi K., Wakiwaka H., Yamada H., "Consideration on the angular error due to the shaft eccentricity and the compensation effect by short-circuit winding on a resolver," *J. Magn. Soc. Jpn.* 22, pp. 701-704, 1998.
- [14] Krause P. C., *Analysis of Electrical Machinery*, McGraw-Hill series in electrical engineering, Power & energy, 1986.
- [15] Ong C., *Dynamic Simulation of Electric Machinery Using Matlab/Simulink*, Prentice Hall PTR. Upper Saddle River, New Jersey, 1998.
- [16] R/D datasheets of Analog Device Company; presented at <http://www.analog.com>; received at 2007-02.



Davood Arab-Khaburi was born in 1965. He has received B.Sc. in 1990 from Sharif University of Technology in Electronic Engineering and M.Sc. and Ph.D. from ENSEM INPEL, Nancy, France in 1994 and 1998, respectively. He has joined to UTC in Compiègne, France (1998-1999). Since 2000 he has been as a faculty member of Iran University of Science and Technology. His research interests are Power Electronic and Motor Control.



Farid Tootoonchian has received his B.Sc. and M.Sc. degrees in Electrical Engineering from the Iran University of Sciences and Technology, Tehran, Iran in 2000 & 2007 respectively. He has done over 22 industrial projects including one national project, held 5 patents, published more than 8 journal and 22 conference papers about electrical machines and sensors over the years. His research interest is design of small electromagnetic measurement machines and sensors.



Zahra Nasiri-Gheidari has received her B.Sc. degree in Electrical Engineering from the Iran University of Science and Technology, Tehran, Iran in 2004. And she received the Master degree in Electrical Power Engineering from the University of Tehran in 2006, graduating with First Class Honors in both of them. She is

currently director of the Electrical machines Lab. in the Electrical Engineering Department of Sharif University of Technology, Tehran, Iran. Her research interests are design and modeling of electrical machines and drives.